Chemistry of Metals and Alloys

Chem. Met. Alloys 6 (2013) 125-129
Ivan Franko National University of Lviv
www.chemetal-journal.org

Interactions in the ternary reciprocal system Tl_2S+SnTe↔Tl_2Te+SnS

M.J. FILEP[1]*, M.Yu. SABOV[1], I.E. BARCHIY[1], K.J. PLUCINSKI[2], A.M. SOLOMON[3]

[1] *Faculty of Chemistry, Uzhhorod National University, Pidhirna St. 46, 88000 Uzhhorod, Ukraine*
[2] *Department of Electronics, Military University of Technology, Kaliskiego 2, 00-908 Warsaw, Poland*
[3] *Institute of Electron Physics, Universytetska St. 21, 88017 Uzhhorod, Ukraine*
* *Corresponding author. Tel.: +380-312-237163; fax: +380-312-235091; e-mail: mfilep23@mail.ru*

Received September 20, 2013; accepted December 25, 2013; available on-line August 30, 2014

The phase diagram of the ternary reciprocal system Tl_2S+SnTe↔Tl_2Te+SnS was investigated using differential-thermal analysis, X-ray diffraction and microstructure analysis. The liquidus surface projection, the isothermal section at 520 K and phase diagrams of four vertical sections were constructed. The liquidus consists of seven primary crystallization fields. The extent of the continuous solid solution range based on the ternary phase Tl_4SnTe_3 was estimated.

Thermal analysis / X-ray diffraction/ Microstructure analysis/ Phase diagram / Isothermal section / Solid solution

Introduction

The Tl_4XY_3 (X = Sn, Pb; Y = S, Se, Te) compounds are characterized by low thermal conductivity and relatively high thermoelectric figures of merit *ZT* [1]. Therefore the $Tl_4SnS_3(Te_3)$ compounds can be considered as perspective materials for thermoelectric devices. To increase the scope of their use, an investigation of the physico-chemical interaction in systems based on the compounds $Tl_4SnS_3(Te_3)$ seemed promising. The two ternary compounds crystallize in isotypic tetragonal structures [2,3], which indicates a high probability of formation of a solid solution.

Experimental

Binary thallium(I) and tin(II) sulfides and tellurides were prepared from stoichiometric amounts of high-purity initial elements (99.99 wt.%) in evacuated quartz ampoules. The Tl_4SnS_3, Tl_4SnTe_3 and $Tl_2Sn_2S_3$ ternary compounds were obtained from stoichiometric amounts of binary Tl_2S, SnS and SnTe. Multicomponent alloys were synthesized by the direct single-temperature method from binary and ternary sulfides and tellurides in quartz ampoules, which were evacuated to a residual pressure of 0.13 Pa. The highest synthesis temperature was 920 K. After thermal treatment at the highest temperature for 24-36 h the samples were slowly cooled (20-30 K per hour) down to 520 K and homogenized at this temperature for 168 h. Subsequently the ampoules were quenched in cold water. The phase equilibria were studied by differential thermal analysis (DTA) and X-ray powder diffraction in combination with the simplex method of mathematical modeling of phase equilibria in multicomponent systems. The differential thermal analysis was carried out by means of a device including an *x-y* recorder PDA-1 and a chromel-alumel thermocouple (the linearity of heating and cooling was controlled by a RIF-101 programmer), with an accuracy of ±5 K. X-ray powder diffraction data was collected on a DRON-4 diffractometer (Cu *K*α radiation, Ni filter). The microstructure analysis was carried out with a metallographic microscope Lomo Metam R1. The simplex method of computer simulation of phase equilibria is described in [4].

Results and discussion

The Tl_2S–Tl_2Te [5] and SnS–SnTe [6] systems are of the eutectic type; also in the SnS–SnTe system a eutectoid process takes place (based on the polymorphic transformation of SnS) [6]. The quasi-binary systems Tl_2S–SnS [7] and Tl_2Te–SnTe [8,9] are characterized by the formation of one congruently melting ternary compound: Tl_4SnTe_3 (817 K), and two incongruently melting compounds: Tl_4SnS_3 (626 K) and $Tl_2Sn_2S_3$ (679 K). A continuous series of solid solutions is formed between the binary thallium(I) telluride and Tl_4SnTe_3.

The Tl_4SnTe_3 ternary compound, which melts congruently, exists on one of the sides of the $Tl_2S+SnTe \leftrightarrow Tl_2Te+SnS$ system. Therefore, it may be that none of the Tl_2S–SnTe or Tl_2Te–SnS diagonals of the quadrangle will be stable and the stable sections could be formed by Tl_4SnTe_3 (Fig. 1). For this reason the quasibinary sections of the reciprocal $Tl_2S+SnTe \leftrightarrow Tl_2Te+SnS$ system must be determined first.

The determination of the quasibinary sections was carried out by phase analysis of samples lying at the intersection of possible quasibinary sections [10]. Three points of intersection of possible quasibinary sections exist in the reciprocal system $Tl_2S+SnTe \leftrightarrow Tl_2T+SnSe$ (Fig. 1). For the determination of the quasibinary sections, alloys corresponding to points 1 and 3 were synthesized and investigated by XRD and microstructure analysis. Based on the results, quasibinarity was established for the two sections (Tl_2S–Tl_4SnTe_3, SnSe–Tl_4SnTe_3).

The Tl_2S–Tl_4SnTe_3 system belongs to the Rozeboom type V (Fig. 2). The system liquidus consists of two parts: the primary crystallization of solid solutions based on Tl_2S and Tl_4SnTe_3 crystals. The coordinates of the eutectic point are 82 mol.% Tl_2S, 605 K (eutectic process $L \leftrightarrow Tl_2S+Tl_4SnTe_3$). At the annealing temperature (520 K) the solid solution ranges of Tl_2S and Tl_4SnTe_3 do not exceed 10 and 65 mol.%, respectively. The formation of a wide region of solid solution based on the Tl_4SnTe_3 phase was confirmed by the change of the cell parameters according to Vegard's law. Within the solid solution range the lattice parameters change from a = 8.819 Å, c = 13.013 Å for Tl_4SnTe_3 to a = 8.836 Å, c = 12.906 Å for the boundary solid solution (Fig. 3). The results of the microstructure analysis support the XRD data on the phase composition in the system Tl_2S–Tl_4SnTe_3.

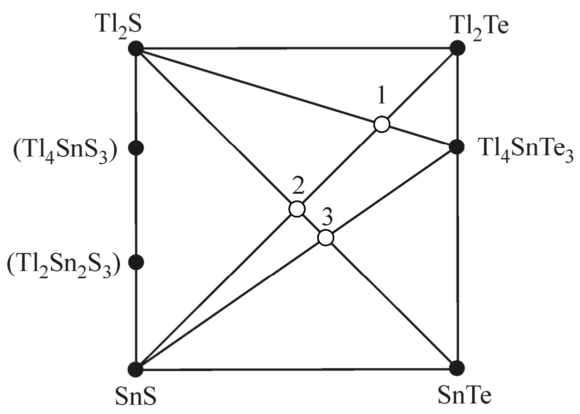

Fig. 1 Possible quasibinary sections in the reciprocal system $Tl_2S+SnTe \leftrightarrow Tl_2Te+SnS$.

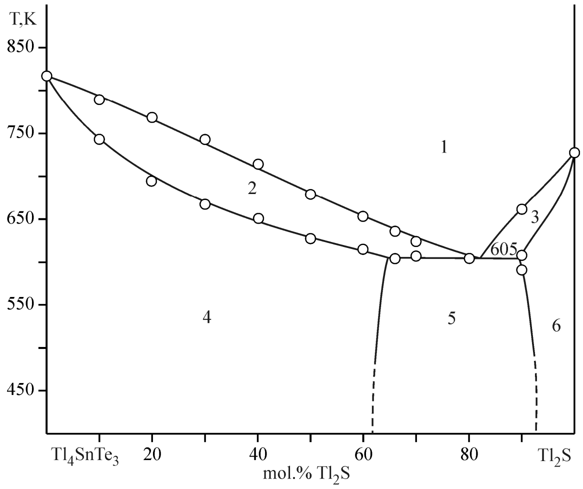

Fig. 2 Phase diagram of the Tl_2S–Tl_4SnTe_3 system: 1 – L, 2 – L+Tl_4SnTe_3, 3 – L+Tl_2S, 4 – [Tl_4SnTe_3], 5 – Tl_2S+Tl_4SnTe_3, 6 – [Tl_2S].

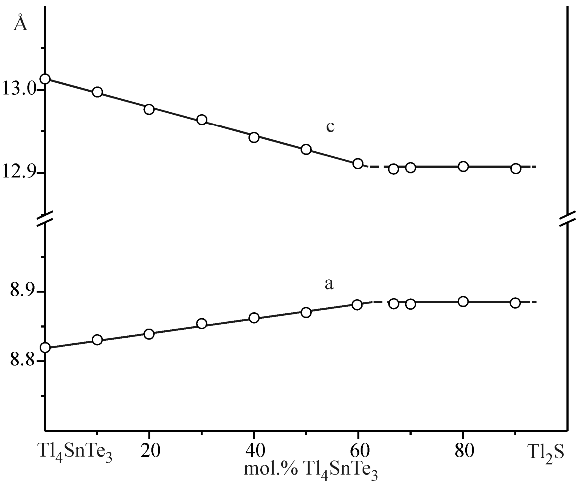

Fig. 3 Lattice parameters of Tl_4SnTe_3 in the system Tl_2S–Tl_4SnTe_3.

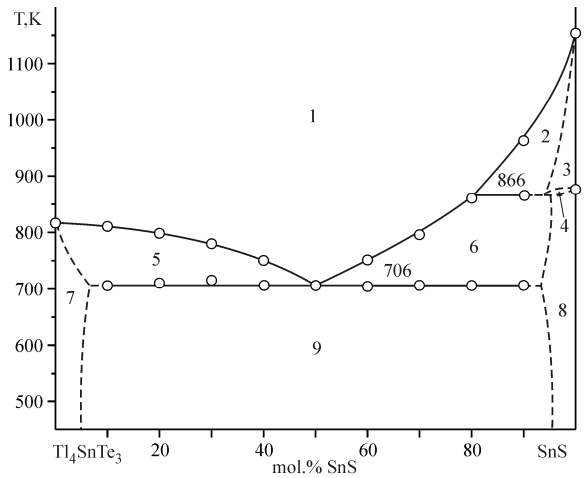

Fig. 4 Phase diagram of the SnS–Tl_4SnTe_3 system: 1 – L, 2 – L+ht-SnS, 3 – [ht-SnS], 4 – ht-SnS+lt-SnS, 5 – L+Tl_4SnTe_3, 6 – L+lt-SnS, 7 – [Tl_4SnTe_3], 8 – [lt-SnS], 9 – lt-SnS+Tl_4SnTe_3.

The phase diagram of the $SnS–Tl_4SnTe_3$ system is presented in Fig. 4. The liquidus of the quasibinary system consists of three lines of primary crystallization, which cross in two invariant points with the following coordinates: 50 mol.% SnS, 706 K (eutectic process $L \leftrightarrow$lt-SnS+Tl_4SnTe_3) and 81 mol.% SnS, 866 K (metatectic process ht-SnS$\leftrightarrow$L+lt-SnS). The solid solution ranges based on Tl_4SnTe_3 and lt-SnS do not exceed 5 mol.%. at 520 K.

The $Tl_2Sn_2S_3–Tl_4SnTe_3$ and $Tl_4SnS_3–Tl_4SnTe_3$ systems are non-quasibinary above the solidus, due to the incongruent melting of the $Tl_2Sn_2S_3$ and Tl_4SnS_3 compounds.

The vertical section of the $Tl_2Sn_2S_3–Tl_4SnTe_3$ system is presented in Fig. 5. The liquidus consists of two lines that belong to the fields of primary crystallization of Tl_4SnTe_3 and lt-SnS, which participates in the peritectic process of formation of $Tl_2Sn_2S_3$. The lines of primary crystallization intersect in the point with the coordinates 79 mol.% $Tl_2Sn_2S_3$, 626 K. The fields of primary crystallization are separated by a three-phase field, L+lt-SnS+Tl_4SnTe_3. At the annealing temperature (520 K) the solid solution ranges of Tl_4SnTe_3 and $Tl_2Sn_2S_3$ do not exceed 50 and 5 mol.%, respectively. The formation of a wide region of solid solution based on the Tl_4SnTe_3 phase is confirmed by the change of the cell parameters according to Vegard's law. The lattice parameters within the solid solution range change from a = 8.819 Å, c = 13.013 Å for Tl_4SnTe_3 to a = 8.864 Å, c = 12.933 Å for the boundary solid solution (Fig. 6).

The vertical section of the $Tl_4SnS_3–Tl_4SnTe_3$ system is presented in Fig. 7. The liquidus consists of two lines that belong to the fields of primary crystallization of Tl_4SnTe_3 and Tl_2S, which participates in the peritectic process of formation of the Tl_4SnS_3 phase. The lines of primary crystallization intersect in the point with the coordinates 83 mol.% Tl_4SnS_3, 600 K. The fields of primary crystallization are separated by the three-phase field L+Tl_2S+Tl_4SnTe_3. The $Tl_4SnS_3–Tl_4SnTe_3$ system is the connecting line of the quasiternary system $Tl_2S–Tl_4SnTe_3–SnS$. It divides the fields of completion of secondary crystallization. This explains the fact that the three-phase region L+Tl_2S+ht-Tl_4SnS_3 borders the single-phase region ht-Tl_4SnS_3. At 520 K the extents of the solid solution ranges based on Tl_4SnTe_3 and lt-Tl_4SnS_3 are less than 20 and 10 mol.%, respectively.

The isothermal section of the $Tl_2S+SnTe \leftrightarrow Tl_2Te+SnS$ system includes six single-phase solid solution ranges; four are located in the corners of a quadrangle and two are located between the binary sulfides (Fig. 8).

A projection of the liquidus surface of the reciprocal system $Tl_2S+SnTe \leftrightarrow Tl_2Te+SnS$ (Fig. 9) onto the concentration quadrangle was constructed according to the results of the DTA investigation and a computer simulation of the phase equilibria in

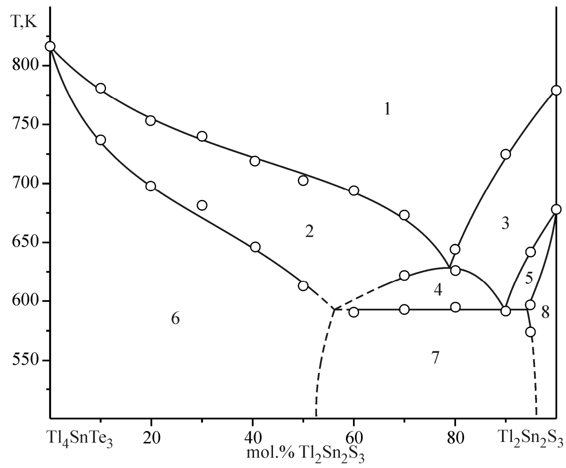

Fig. 5 Phase diagram of the $Tl_2Sn_2S_3–Tl_4SnTe_3$system: 1 – L, 2 – L+Tl_4SnTe_3, 3 – L+lt-SnS, 4 – L+lt-SnS+Tl_4SnTe_3, 5 – L+lt-SnS+$Tl_2Sn_2S_3$, 6 – [Tl_4SnTe_3], 7 – $Tl_2Sn_2S_3$+Tl_4SnTe_3, 8 – [$Tl_2Sn_2S_3$].

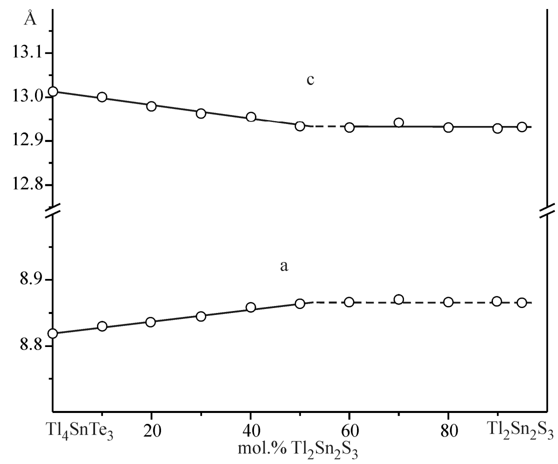

Fig. 6 Lattice parameters of Tl_4SnTe_3 in the system $Tl_2Sn_2S_3–Tl_4SnTe_3$.

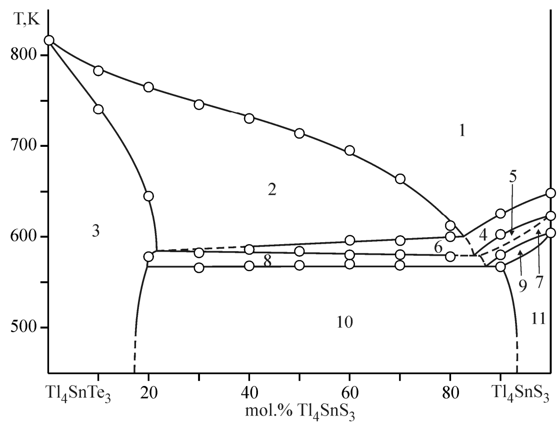

Fig. 7 Phase diagram of the $Tl_4SnS_3–Tl_4SnTe_3$ system: 1 – L, 2 – L+Tl_4SnTe_3, 3 – [Tl_4SnTe_3], 4 – L+Tl_2S, 5 – L+Tl_2S+ht-Tl_4SnS_3, 6 – L+Tl_2S+Tl_4SnTe_3, 7 – [ht-Tl_4SnS_3], 8 – Tl_4SnTe_3+ht-Tl_4SnS_3, 9 – ht-Tl_4SnS_3+lt-Tl_4SnS_3, 10 – Tl_4SnTe_3+lt-Tl_4SnS_3, 11 – [lt-Tl_4SnS_3].

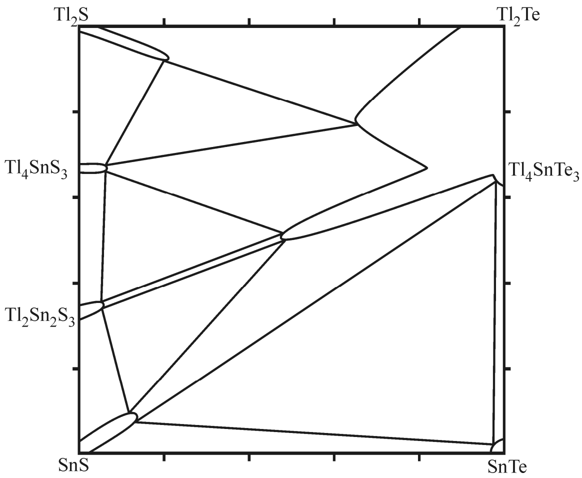

Fig. 8 Isothermal section of the reciprocal system Tl_2S+SnTe↔Tl_2Te+SnS at 520 K.

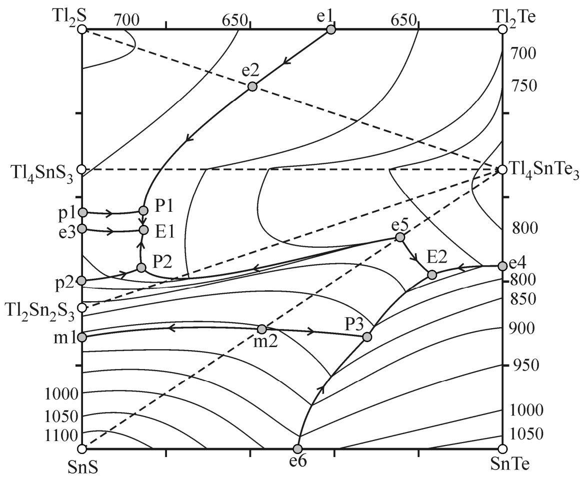

Fig. 9 Projection of the liquidus surface of the reciprocal system Tl_2S+SnTe↔Tl_2Te+SnS.

multicomponent systems by the simplex method. It consists of seven fields of primary crystallization: Tl_2S (Tl_2S-e1-e2-P1-p1-Tl_2S), the solid solution based on Tl_2Te and Tl_4SnTe_3 (Tl_2Te-Tl_4SnTe_3-e4-E2-e5-P2-E1-P1-e2-e1-Tl_2Te), ht-Tl_4SnS_3 (p1-P1-E1-e3-p1), $Tl_2Sn_2S_3$ (p2-e3-E1-P2-p2), lt-SnS (m1-p2-P2-e5-E2-P3-m2-m1), ht-SnS (SnS-m1-m2-P3-e6-SnS), and SnTe (SnTe-e6-P3-E2-e4-SnTe). The fields of primary crystallization are divided by 14 monovariant eutectic, peritectic and metatectic lines. The types and temperatures of the processes in the reciprocal system Tl_2S+SnTe↔Tl_2Te+SnS are shown in Table 1.

The monovariant lines cross in three invariant peritectic and two invariant eutectic points:

P1: L+Tl_2S↔Tl_4SnTe_3+ht-Tl_4SnS_3; 60 mol.% 3Tl_2S, 18 mol.% Tl_4SnTe_3, 22 mol.% 3SnS, 600 K;

P2: L+lt-SnS↔$Tl_2Sn_2S_3$+Tl_4SnTe_3; 31 mol.% 3Tl_2S, 20 mol.% Tl_4SnTe_3, 49 mol.% 3SnS, 621 K;

P3: L+SnTe↔lt-SnS+Tl_4SnTe_3; 44 mol.% 3SnS, 20 mol.% Tl_4SnTe_3, 36 mol.% 3SnTe, 816 K;

E1: L↔ht-Tl_4SnS_3+$Tl_2Sn_2S_3$+Tl_4SnTe_3; 43 mol.% 3Tl_2S, 17 mol.% Tl_4SnTe_3, 40 mol.% 3SnS, 590 K;

E2: L↔lt-SnS+SnTe+Tl_4SnTe_3; 35 mol.% 3SnS, 36 mol.% Tl_4SnTe_3, 29 mol.% 3SnTe, 700 K.

New complex compounds were not observed in the reciprocal system Tl_2S+SnTe↔Tl_2Te+SnS.

Conclusions

The physico-chemical interactions in the reciprocal system Tl_2S+SnTe↔Tl_2Te+SnS were for the first time investigated by differential thermal and microstructure analysis, X-ray powder diffraction and mathematical simulation of phase equilibria in multicomponent systems by the simplex method. The character of the monovariant processes and the temperatures and coordinates of the invariant processes were determined. The existence of solid solutions of the ternary compounds Tl_4SnS_3 and Tl_4SnTe_3 was established.

Table 1 Type and temperature of the processes in the reciprocal system Tl_2S+SnTe↔Tl_2Te+SnS.

Monovariant line	Process	Temperature, K
e1-e2	L↔Tl_2S+[Tl_2Te+Tl_4SnTe_3]	628-605
e2-P1	L↔Tl_2S+Tl_4SnTe_3	605-600
p1-P1	L+Tl_2S↔ht-Tl_4SnS_3	626-600
P1-E1	L+Tl_2S↔ht-Tl_4SnS_3+Tl_4SnTe_3	600-590
e3-E1	L↔ht-Tl_4SnS_3+$Tl_2Sn_2S_3$	613-590
e5-P2	L↔lt-SnS+Tl_4SnTe_3	706-621
p2-P2	L+lt-SnS↔$Tl_2Sn_2S_3$	679-621
P2-E1	L+lt-SnS↔$Tl_2Sn_2S_3$+Tl_4SnTe_3	621-590
m2-m1	ht-SnS↔L+lt-SnS	866-864
m2-P3	ht-SnS↔L+lt-SnS	866-816
e6-P3	L↔ht-SnS+SnTe	973-816
e5-E2	L↔lt-SnS+Tl_4SnTe_3	706-700
e4-E2	L↔SnTe+Tl_4SnTe_3	773-700
P3-E2	L+ht-SnS↔lt-SnS+SnTe	739-730

References

[1] A. Kosuga, K. Kurosaki, H. Muta, S. Yamanaka, *MRS Online Proc. Libr.* 886 (2006) 063705 (4 p.).
[2] S. Del Bucchia, J.C. Jumas, E. Philippot, M. Maurin, *Rev. Chim. Min.* 18 (1981) 224-234.
[3] S. Bradtmöller, P. Böttcher, *Z. Anorg. Allg. Chem.* 619 (1993) 1155-1160.
[4] I.E. Barchiy, *Ukr. Khim. Zh*. 67 (2001) 18.
[5] M.M. Asadov, M.B. Babanly, A.A. Kuliev, *Izv. Akad. Nauk SSSR, Neorg. Mater*. 13(8) (1977) 1520-1521.
[6] A.A. Volykhov, V.I. Shtanov, L.V. Yashina, *Inorg. Mater*. 44(4) (2008) 345-356.
[7] T.A. Malakhovskaya-Rosokha, M.Yu. Sabov, I.E. Barchiy, E.Yu. Peresh, *Zh. Neorg. Khim*. 56(1) (2011) 122-127.
[8] W. Gawel, E. Zaleska, E. Maskievicz, *J. Therm. Anal*. 36 (1990) 2323-2327.
[9] T.A. Malakhovska-Rosokha, *Nauk. Visn. Uzhhorod. Univ., Ser. Khim.* 2(26) (2011) 16-18.
[10] I.E. Barchiy, E.Yu. Peresh, V.M. Rizak, V.O. Khudolij, *Heterogeneous Equilibrium*, Zakarpattya, Uzhhorod, 2003 (in Ukrainian).